Pergamon

Tetrahedron 56 (2000) 9819–9831

TETRAHEDRON

Synthesis, Biological Activities and Conformational Studies of Somatostatin Analogs

Ralph-Heiko Mattern, Sandra Blaj Moore, Thuy-Anh Tran, Jaimie K. Rueter and Murray Goodman*

Department of Chemistry and Biochemistry, University of California at San Diego, La Jolla, CA 92093-0343, USA

Received 19 May 2000; accepted 17 August 2000

Abstract—We review our recent studies on synthesis, conformational analysis and biological activity of a series of analogs of the cyclic hexapeptide L-363,301 c-[Phe[11]-Pro[6]-Phe[7]-D-Trp[8]-Lys[9]-Thr[10]] and of analogs of the cyclic octapeptide D-Phe[5]-c[Cys[6]-Phe[7]-D-Trp[8]-Lys[9]-Thr[10]-Cys[11]]-Thr[12]-ol (sandostatin®, octreotide). The proline residue in L-363,301 was substituted with *N*-alkylated glycine residues resulting in a series of compounds with the general structure c-[Xaa[11]-Nxbb[6]-Xcc[7]-D-Trp[8]-Lys[9]-Thr[10]] (the numbering refers to the positions of the residues in native somatostatin) with Xaa=Phe or Nal, Xcc=Phe or Nal and Nxbb=**Nphe** (*N*-benzylglycine), **(*R*)-β-MeNphe** ([*N*-(*R*)α-methylbenzyl]glycine), **(*S*)-β-MeNphe** ([*N*-(*S*)α-methylbenzyl]glycine), **Nnal** [*N*-(naphthylmethyl)glycine], **Nasp** [*N*-(2-carboxyethyl)glycine], **Nlys** [*N*-(4-aminobutyl)glycine], **Ndab** [N-(2-aminoethyl)glycine]. These compounds were used to investigate the effect of different substitutions within the bridging region of L-363,301 and our studies resulted in compounds that exhibit increased selectivity toward the hsst2 receptor compared to the parent compound. The sandostatin analogs D-Phe[5]-c[Cys[6]-Phe[7]-D-Trp[8]-Lys[9]-Thr[10]-Cys[11]]-Thr[12]-NH_2 (Xaa=allo-Thr, D-allo-Thr, D-βHyv (D-β-hydroxyvaline), L-βHyv (L-β-hydroxyvaline), D-Thr and Xbb=Thr or Xaa=Thr and Xbb=allo-Thr, D-allo-Thr, L-βHyv, D-Thr) contain subtle stereochemical changes in the Thr residues in positions 10 and 12. These changes enabled us to investigate the influence of the stereochemistry within these residues on conformation and binding affinity. The compounds with (*S*)-configuration at the C^{α} of residue 10 exhibit binding to the hsst receptors and adopt conformations containing a type II′ β-turn spanning residues D-Trp and Lys while those compounds with (*R*)-configuration at the C^{α} of residue 10 are inactive and adopt different backbone conformations.

Introduction

The peptide hormone somatostatin, a disulfide bridged tetradecapeptide is a regulatory hormone with significant physiological roles as an inhibitor of the release of several other hormones (e.g. glucagon, growth hormone, insulin, gastrin).[1–3] Somatostatin agonists are pharmacologically interesting targets for the treatment of diseases such as acromegaly, cancer, diabetes, rheumatoid arthritis and Alzheimer's. Somatostatin interacts with G protein-coupled receptors, and five human subtypes (hsst1–5) have been cloned and characterized.[4] It has been shown that hsst2 mediates the antiproliferative effects of the hormone thus making the hsst2 receptor a potentially important target for cancer therapy.[5] The hsst5 receptor is believed to be responsible for inhibition of insulin release and could be useful in the treatment of insulin-dependent diabetes.[6] It has been suggested that the hsst3 receptor plays a role in the observed somatostatin-mediated inhibition of gastric acid and acetylcholine release.[7]

Extensive structure–activity relationship studies led to the discovery of several highly potent somatostatin analogs such as the cyclic hexapeptide c-[Pro[6]-Phe[7]-D-Trp[8]-Lys[9]-Thr[10]-Phe[11]] (L-363,301) by Veber and coworkers[8] (the numbering refers to the location of the residues in native somatostatin) and the cyclic octapeptide D-Phe[5]-c[Cys[6]-Phe[7]-D-Trp[8]-Lys[9]-Thr[10]-Cys[11]]-Thr[12]-ol (SMS 201-995, sandostatin® or octreotide) by Bauer et al.[9] (the numbering of the residues in L-363,301 is maintained).

Since the discovery of L-363,301 by the Merck group and sandostatin (octreotide) by Sandoz researchers, numerous somatostatin analogs have been synthesized and their conformations in solution have been studied.[9–13] It has been demonstrated that L-363,301 and sandostatin share common structural motifs such as a type II′ β-turn with D-Trp-in the $i+1$ position and a type VI β-turn in the so-called bridging region Xaa[11]-Xbb[6] characterized by a *cis* peptide bond or mimicked by a disulfide or lanthionine bridge as in sandostatin analogs.[10–13]

It has been postulated that the tetrapeptide sequence Phe[7]-D-Trp[8]-Lys[9]-Thr[10] is the biologically active portion, interacting with the receptor, while the Xaa[11]-Xbb[6] sequence is important for maintaining the proper orientation of the

Keywords: somatostatin analogs; hsst2; Nphe.

* Corresponding author. Tel.: +619-534-4466; fax: +619-534-0202; e-mail: mgoodman@ucsd.edu

0040–4020/00/$ - see front matter
PII: S0040-4020(00)00889-9

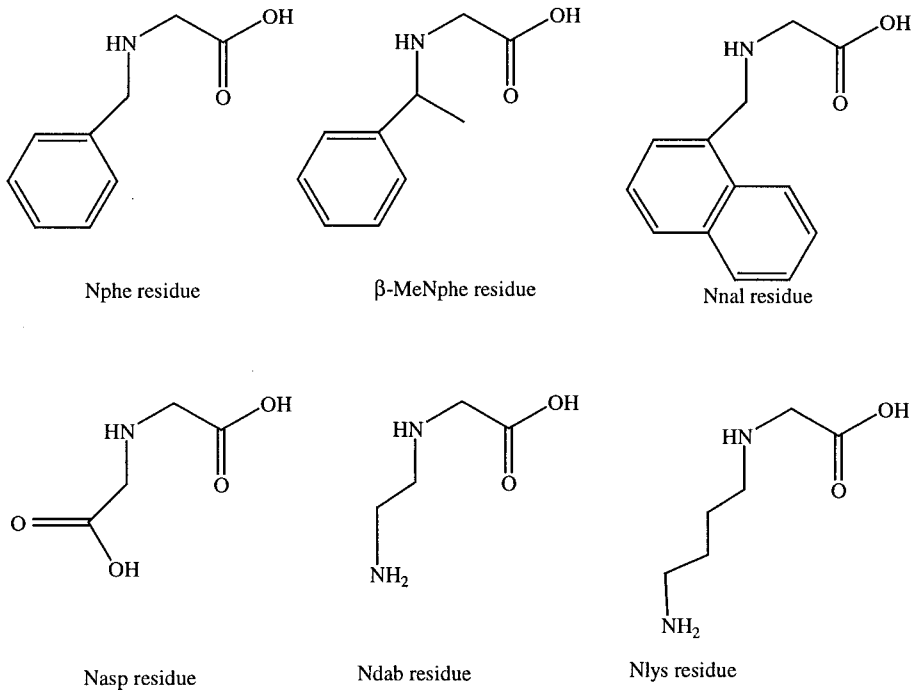

Figure 1. The structures of the *N*-alkylated glycine residues incorporated into L-363,301.

tetrapeptide portion. Conformational studies on L-363,301 have also shown that the molecule adopts two backbone conformations which are both consistent with all NMR data: a 'flat' conformation and a conformation which is 'folded' about Phe[7] and Thr[13].[16]

The conformational analysis of a series of α- and β-methylated analogs of L-363,301 revealed valuable information regarding the 'bioactive' conformation of the side chains and of the backbone conformation by restricting the conformational flexibility of these analogs compared to the parent compound **1**.[14,15] It was deduced from these studies that the 'folded' and not the 'flat' conformation might be the 'bioactive' conformation.

The conformations in solution of sandostatin® and its analogs were subject of numerous investigations. Studies by Van Binst et al.[16–18] and others using ^{1}H NMR have demonstrated that sandostatin and active analogs adopt predominantly an antiparallel β-sheet conformation with a type II′ β-turn spanning residues D-Trp and Lys. Experimental data suggest that the antiparallel β-sheet cannot be the only accessible conformation. The Phe[3]NH proton in such a β-sheet structure is involved in a hydrogen bond with Thr[6]C=O and neither in sandostatin nor in its analogs is the temperature coefficient of this NH-proton low enough to account for a stable hydrogen bond involving this proton. Furthermore, certain NOEs observable for sandostatin cannot be explained by a single β-sheet structure. The results of X-ray diffraction studies on sandostatin[19] have shown that this molecule adopts three structures in the crystalline state, one of which corresponds to the structure observed in solution. In the other two structures the C-terminal tripeptide portion of the molecule adopts a helical fold. Extensive studies by ^{1}H NMR and molecular modeling and comparison with the crystal structures have suggested that sandostatin® exists in a conformational equilibrium between multiple structures in fast exchange. By assuming an equilibrium between antiparallel β-sheet structures and conformations in which the C-terminal portion forms a 3^{10} helix-like fold similar to the conformations observed in the solid state it was possible to explain the NMR data which were not consistent with the antiparallel β-sheet structure.[20]

In this paper we summarize the results of synthesis, binding studies to the hsst receptor and conformational analyses of analogs of L-363,301 containing *N*-alkylated residues and of sandostatin analogs containing subtle stereochemical changes in the residues 6 or 8.[21–28]

As part of our efforts to investigate the role of the bridging region in cyclic hexapeptide analogs of somatostatin we substituted the proline residue in c-[Phe[11]-Pro[6]-Phe[7]-D-Trp[8]-Lys[9]-Thr[10]] (**1**) L-363,301 with *N*-alkylated glycine residues. A series of analogs of L-363,301 with the general structure c-[Xaa[11]-Nxbb[6]-Xcc[7]-D-Trp[8]-Lys[9]-Thr[10]] with Xaa=Phe or Nal, Xcc=Phe or Nal and Nxbb=Nphe, (*R*)-β-Methyl-Nphe, (*S*)-β-Methyl-Nphe, Nnal, Nasp, Nlys, Ndab was designed, synthesized and tested for binding to the isolated human somatostatin receptors. The structures of the peptoid residues are shown in Fig. 1. The sequence of the peptides and their denotations are given in Table 1.

The sandostatin analogs D-Phe[1]-c[Cys[2]-Phe[3]-D-Trp[4]-Lys[5]-Xaa[6]-Cys[7]]-Xbb[8]-NH_2 (Xaa=allo-Thr, D-allo-Thr, D-βHyv, β Hyv, D-Thr and Xbb=Thr or Xaa=Thr and Xbb=allo-Thr, D-allo-Thr, β Hyv, D-Thr) contain subtle stereochemical changes in the Thr residues in positions 6 and 8.

Table 1. Peptoid analogs of L-363,301

Compound	Abbreviation
c-[Phe^{11}-Nphe^{6}-Phe^{7}-D-Trp^{8}-Lys^{9}-Thr^{10}]	**Nphe analog**
c-[Phe^{11}-Nnal^{6}-Phe^{7}-D-Trp^{8}-Lys^{9}-Thr^{10}]	**Nnal analog**
c-[Phe^{11}-Nphe^{6}-Nal^{7}-D-Trp^{8}-Lys^{9}-Thr^{10}]	**Nphe-Nal analog**
c-[Nal^{11}-Nphe^{6}-Phe^{7}-D-Trp^{8}-Lys^{9}-Thr^{10}]	**Nal-Nphe analog**
c-[Phe^{11}-(*R*)-βMeNphe^{6}-Phe^{7}-D-Trp^{8}-Lys^{9}-Thr^{10}]	**(*R*)-βMeNphe analog**
c-[Phe^{11}-(*S*)-βMeNphe^{6}-Phe^{7}-D-Trp^{8}-Lys^{9}-Thr^{10}]	**(*S*)-βMeNphe analog**
c-[Phe^{11}-(*R*)-βMeNphe^{6}-Nal^{7}-D-Trp^{8}-Lys^{9}-Thr^{10}]	**(*R*)-βMeNphe^{-}Nal analog**
c-[Phe^{11}-(*S*)-βMeNphe^{6}-Nal^{7}-D-Trp^{8}-Lys^{9}-Thr^{10}]	**(*S*)-βMeNphe^{-}Nal analog**
c-[Nal^{11}-(*R*)-βMeNphe^{6}-Phe^{7}-D-Trp^{8}-Lys^{9}-Thr^{10}]	**Nal-(*R*)-βMeNphe analog**
c-[Nal^{11}-(*S*)-βMeNphe^{6}-Phe^{7}-D-Trp^{8}-Lys^{9}-Thr^{10}]	**Nal-(*S*)-βMeNphe analog**
c-[Phe^{11}-Nasp^{6}-Phe^{7}-D-Trp^{8}-Lys^{9}-Thr^{10}]	**Nasp analog**
c-[Phe^{11}-Ndab^{6}-Phe^{7}-D-Trp^{8}-Lys^{9}-Thr^{10}]	**Ndab analog**
c-[Phe^{11}-Nlys^{6}-Phe^{7}-D-Trp^{8}-Lys^{9}-Thr^{10}]	**Nlys analog**

Cyclic Hexapeptides Related to L-363,301

The *N*-alkylated residues were synthesized in solution starting from appropriately protected bromoacetic acid (ethyl or benzyl) and the appropriate amine. The Nasp residue was synthesized in solution from glycine benzyl ester and *tert*-butyl bromoacetate to give the fully protected Nasp residue. The Ndab and Nlys residues were prepared from Boc-monoprotected amines and benzyl bromoacetate. The Nphe, (*R*)-β-MeNphe, (*S*)-β-MeNphe and Nnal were synthesized from ethyl bromoacetate and the appropriate arylalkyl amines. The synthesis of the cyclic hexapeptides was designed around the fragment condensation of the appropriately protected tripeptide sequence Xaa-Nxbb-Xcc-OBzl with the tripeptide Cbz-D-Trp-Lys(Boc)-Thr-(*t*Bu)-OH to afford the protected linear hexapeptide Cbz-D-Trp-Lys(Boc)-Thr-(*t*Bu)-Xaa-Nxbb-Xcc-OBzl which was subjected to hydrogenation to remove the N- and C-terminal protecting groups. Cyclization with DPPA/K_2HPO_4 at 1 mMol concentration in DMF followed by treatment with TFA in the presence of scavengers afforded the cyclic hexapeptide in good overall yields. The synthesis of c-[Phe^{11}-(*R*)βMeNphe^{6}-Phe^{7}-D-Trp^{8}-Lys^{9}-Thr^{10}] is shown in Fig. 2 as a representative example.

The somatostatin analogs were tested in vitro for their specific binding to the five human somatostatin receptor subtypes expressed in CHO cell lines and are compared to L-363,301 as shown in Table 2. The incorporation of the peptoid residue Nphe into position 6 resulted in the **Nphe** compound which is more selective towards hsst2 compared with L-363,301. There is a loss in activity in binding towards hsst2 and hsst5 while the activity towards hsst2 remains the same. Introduction of the Nnal residue into that position increased the selectivity and gave rise to a compound with lower binding affinities to all receptors

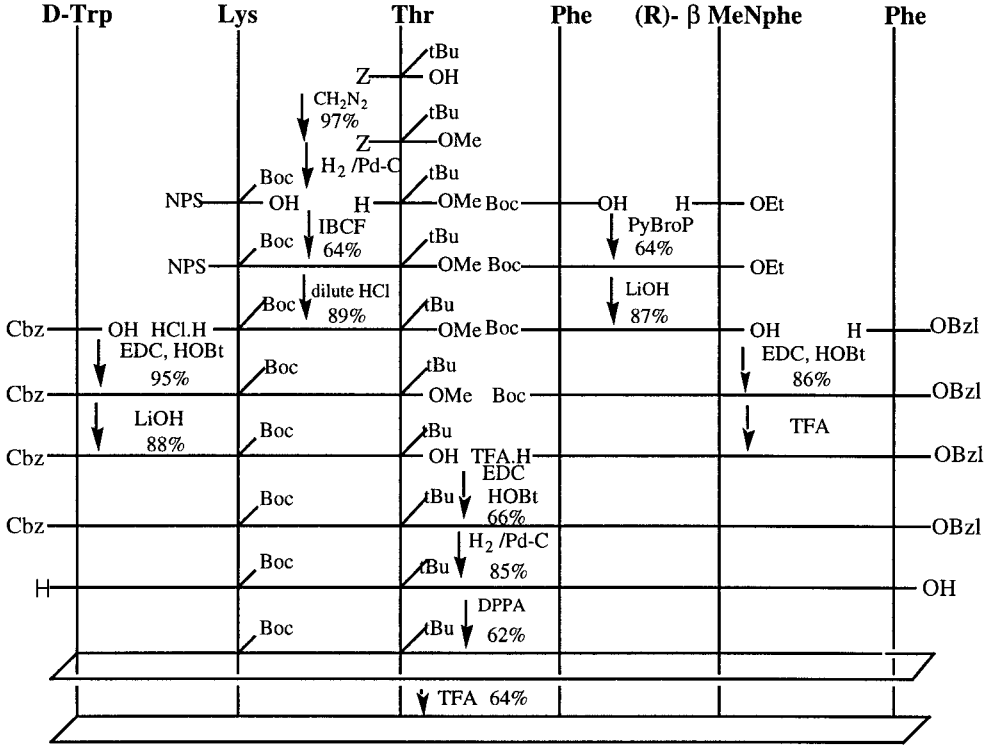

Figure 2. The synthesis of c-[Phe^{11}-(*R*)βMeNphe^{6}-Phe^{7}-D-Trp^{8}-Lys^{9}-Thr^{10}] as a representative example for the synthesis of analogs of L-363,301 containing *N*-alkylated glycine residues.

Table 2. In vitro inhibition of radioligand binding to human recombinant receptors: K_i (nM) ±SEM (binding assays were carried out with cell membranes from CHO-K1 cells)

Compound	hsst1	hsst2	hsst3	hsst4	hsst5
Phe^{11}-Pro^{6}-Phe^{7}	>1000	5.10±0.76	129±51	>1000	20.3±10.5
Phe^{11}-$Nphe^{6}$-Phe^{7}	>1000	6.98±0.83	253±57	>1000	100.7±45.5
Phe^{11}-$Nnal^{6}$-Phe^{7}	>1000	32.2±2.51	>1000	>1000	830±137
Phe^{11}-$Nphe^{6}$-Nal^{7}	>1000	3.57±0.2	204±21.7	>1000	54.2±14.4
Nal^{11}-$Nphe^{6}$-Phe^{7}	>1000	3.73±0.23	88.8±2.4	>1000	24.9±4.4
Phe^{11}-(*R*)-βMeNphe^{6}-Phe^{7}	>1000	2.33±0.41	425±100	>1000	33.5±12.5
Phe^{11}-(*S*)-βMeNphe^{6}-Phe^{7}	>1000	29.5±2.49	797±125	>1000	87±22.6
Phe^{11}-(*R*)-βMeNphe^{6}-Nal^{7}	>1000	7.14±0.16	380±73	>1000	10.3±3.7
Phe^{11}-(*S*)-βMeNphe^{6}-Nal^{7}	>1000	3.15±0.23	198±37	>1000	20.3±10.3
Nal^{11}-(*R*)-βMeNphe^{6}-Phe^{7}	>1000	2.77±0.28	125±7.5	>1000	10.7±3.1
Nal^{11}-(*S*)-βMeNphe^{6}-Phe^{7}	>1000	7.25±2.01	267±58	>1000	27.6±8.5
Phe^{11}-$Nasp^{6}$-Phe^{7}	>1000	157±17	>1000	>1000	>1000
Phe^{11}-$Ndab^{6}$-Phe^{7}	>1000	4.2±0.76	40.4±7.0	>1000	102±33
Phe^{11}-$Nlys^{6}$-Phe^{7}	>1000	4.6±0.08	53.4±8.9	>1000	15.3±3.9

but increased selectivity towards the hsst2 receptor (sevenfold compared to L-363,301 and twofold compared to the **Nphe^{6}** compound). Incorporation of L-naphthylalanine into position 7 or position 11 resulted in the **Nal^{11}-Nphe^{6}** and **Nphe^{6}-Nal^{7}** analogs. The **Nal^{11}-Nphe^{6}** analog binds more effectively to both the hsst3 and hsst5 receptors than the **Nphe^{6}-Nal^{7}** compound and has approximately the same binding activity as L-363,301. The **Nphe^{6}-Nal^{7}** compound is more selective than the **Nphe^{6}** compound and L-363,301 with regard to binding to the hsst2 receptor.

The binding affinities for the β-methylated analogs **(*R*)-βMeNphe^{6}-Nal^{7}**, **(*S*)-βMeNphe^{6}-Nal^{7}**, **Nal^{11}-(*R*)-βMeNphe^{6}**, and **Nal^{11}-(*S*)-βMeNphe^{6}** are presented in Table 2. These results show that the binding affinities to the hsst2 and hsst3 receptors found for the **(*S*)-βMeNphe^{6}** analog is slightly increased if Nal residue was present in position 7 or 11. The binding affinities to the hsst2 receptors of the **(*R*)-βMeNphe^{6}-Nal^{7}** and **Nal^{11}-(*S*)-βMeNphe^{6}** compounds and those for the **(*S*)-βMeNphe^{6}-Nal^{7}** and **Nal^{11}-(*R*)-βMeNphe^{6}** compounds are so similar that it can be speculated that the presence of the Nal residue in either position 11 or 7 together with the different orientations of the aromatic side chain within the peptoid residue in position 6 leads to a very similar topology which influences the binding to the hsst2 receptor. To a lesser extent this can also be observed for the hsst3 receptor. The binding to the hsst5 receptor on the other hand seems to be primarily influenced by the stereochemistry within the peptoid residue since the Nal containing analogs with the same configuration within the peptoid residue show identical binding affinities. Overall the effects observed in the **(*R*)-βMeNphe^{6}** and **(*S*)-βMeNphe^{6}** analogs with Phe residues in positions 7 and 11 have been reduced by incorporating Nal residues into either position 7 or 11. The selectivity for the hsst2 receptor of the **(*R*)-βMeNphe^{6}** analog was lost by incorporation of the bulky Nal residues which suggests that the concurrent presence of the Nal residue in either positions 7 or 11 and a β-methylated peptoid residue leads to conformations with a less defined topochemical array. The hydrophobicity of these residues diminished the biological effect.

The **Nasp^{6}** compound is inactive at the hsst3 and hsst5 receptors and exhibits only weak binding to the hsst2 receptor. The presence of the basic residue in the **Ndab^{6}** analog results in a compound that maintains potent binding to the hsst2 receptor but has reduced binding activity to the hsst5 receptor compared to L-363,301. The introduction of the Nlys residue in **Nlys^{6}** leads to an enhancement of binding potency to the hsst5 receptor compared to the **Ndab^{6}** analog (sevenfold) and L-363,301 (twofold) while maintaining an identical binding potency to the hsst2 compared to these two compounds. Both the **Ndab^{6}** analog and the **Nlys^{6}** analog show increased binding to the hsst3 compared with L-363,301.

For each of the compounds, two sets of NMR data were observable corresponding to the *cis* and *trans* isomers around the Xaa^{11}-$Nxbb^{6}$ bond. Some of the NMR data are summarized in Tables 3 and 4. The ratio of *cis* and *trans* as given in Table 4 demonstrate that the *cis* conformation is preferred except for the compounds containing (*R*)βMeNphe residues in the bridging region. The presence of *cis* and *trans* isomers demonstrates that the backbone of these compounds is more flexible than that of the parent compound L-363,301 with Pro in position 6. For this compound, only the *cis* isomer was observable by NMR. Based on the activity of L-363,301 and many other compounds that have been synthesized and described in the literature it can be assumed that the *cis* conformation and not the *trans* conformation leads to the 'bioactive' conformation. For clarity we will not discuss the structures with *trans* conformation in this paper. For this information, the reader is referred to the original papers.[21–26] The chemical shifts for the *cis* conformations of all compounds are given in Table 3 and there is great similarity in the NMR data for the different compounds.

The backbone conformation and the side chain orientations of the relevant side chains found for L-363,301 are generally maintained in the *cis* isomers of our peptoid analogs. These compounds have a very similar NOE pattern and data such as a medium NOE between Thr NH and Lys NH, a strong sequential NOE between D-$TrpH^{\alpha}$ and LysNH and low temperature coefficients of the ThrNH (Table 4) suggest that the *cis* isomers of all compounds adopt a type II′ β-turn with D-Trp in the i+1 position. The *cis* peptide bond between Xaa^{11} and the peptoid residue suggests the presence of a type VI β-turn in this region. However, the differences in the temperature coefficients of the Xaa^{7}NH as shown in Table 4 indicate that the stability or rigidity of this turn varies among these compounds. The hydrogen bond

Table 3. Proton assignments of peptoid analogs of L-363,301 (chemical shifts are reported in ppm relative to internal DMSO-d_6)

	NPhe^6	(*S*)-βMe-NPhe^6	(*R*)-βMe-NPhe^6	Nphe^6-Nal^7	(*R*)NMePhe^6-Nal^7	(*S*)NMePhe^6-Nal^7	Phe^{11}-Nnal^6	Nal^{11}-(*R*)-NmePhe^6	Nal^{11}-(*S*)-NmePhe^6	Nasp^6	Ndab^6	Nlys^6
						Xaa^{11}						
HN	8.63	8.38	8.34	8.69	8.4	8.46	8.68	8.52	8.52	8.23	8.49	8.44
Hα	4.95	4.43	4.49	4.91	4.45	4.45	4.92	4.67	4.67	4.75	4.74	4.69
Hβ	2.96/2.93	2.88	2.98/2.78	2.99/2.95	2.97/2.82	2.89	2.97/2.93	3.47/3.31	3.47/3.31	2.94/2.75	2.9	2.87
						Nxbb^6						
Hα	4.34/2.86	3.49/3.14	3.61/3.51	4.34/2.84	3.46/3.21	3.51/3.05	4.31/2.98	2.92/2.71	2.92/2.71	4.24/3.55	4.23/3.32	4.11/3.12
Hβ	4.94/3.25	5.63	5.21	4.84/3.30	5.31	5.65	5.28/3.98	5.55	5.55	3.88/3.55		3.44/2.27
others	–	1.24	1.3		1.24	1.2		1.14	1.14		3.72/2.76	1.12
											2.62/2.51	1.26
												2.64
												7.66
						Xcc^7						
HN	7.83	7.77	7.21	8.1	7.4	8.01	7.96	7.73	7.73	7.65	7.71	7.58
Hα	4.65	4.5	4.43	4.72	4.47	4.63	4.58	4.4	4.4	4.69	4.56	4.59
Hβ	2.88/2.78	2.89/2.81	2.38	3.29/–-	2.78	3.49/3.26	2.72/2.64	2.81/2.76	2.81/2.76	2.83/2.73	2.82	2.90/2.79
						D-Trp						
HN	8.5	8.48	8.48	8.41	8.38	8.41	8.44	8.42	8.42	8.54	8.58	8.48
Hα	4.41	4.46	4.42	4.38	4.38	4.45	4.38	4.43	4.43	4.69	4.35	4.42
Hβ	2.97/2.67	2.91/2.58	2.86/2.52	2.88/2.44	2.71/2.18	2.76/2.31	2.97/2.65	2.94/2.58	2.94/2.58	2.94/2.68	2.93/2.64	2.96/2.70
						Lys						
HN	8.58	8.58	8.57	8.51	8.5	8.5	8.56	8.57	8.57	8.52	8.54	8.56
Hα	3.86	3.79	3.79	3.78	3.7	3.71	3.84	3.87	3.87	3.86	3.84	3.85
Hβ	1.68/1.41	1.69/1.40	1.63/1.36	1.65/1.36	1.56/1.27	1.58/1.36	1.67/1.40	1.68/1.42	1.68/1.42	1.67/1.35	1.68/1.36	1.65/1.36
Hγ	0.96	0.95	0.9	0.83	0.73	0.81	0.93	0.95	0.95	0.89	0.92	0.94
Hδ	1.35	1.38	1.31	1.33	1.32	1.31	1.35	1.37	1.37	1.28	1.42	1.39
Hϵ	2.61	2.62	2.6	2.56	2.56	2.58	2.57	2.64	2.64	2.59	2.6	2.69
NH2	7.6	7.6	7.58	7.56	7.54	7.61	7.62	7.63	7.63	7.6	7.65	7.64
						Thr						
HN	7.14	7.08	7.09	7.12	7.06	7.08	7.12	7.16	7.16	7.11	7.07	7.04
Hα	4.34	4.17	4.18	4.33	4.17	4.2	4.33	4.2	4.2	4.19	4.26	4.26
Hβ	3.89	3.95	4.01	3.92	3.98	3.96	3.91	3.99	3.99	3.85	3.86	3.87
Hγ	1.06	1.03	0.97	1.07	0.97	1.01	1.09	1.04	1.04	0.96	0.97	0.98
OH	5.03	–	–	4.96	–	4.86	5.03	–	–	5.16	4.97	–

Table 4. Temperature coefficients and *cis–trans* ratio of peptoid analogs of L-363,301

	NPhe^{6}	NPhe^{6}-Nal	Nal^{11}-NPhe^{6-}	Nnal^{6}	(*R*)-βMe-NPhe^{6}	(*S*)-βMe-NPhe^{6}	(*R*)-βMe-NPhe^{6}-Nal^{7}	(*S*)-βMe-NPhe^{6}-Nal^{7}	Nal^{11}-(*R*)-βMe-NPhe^{6-}	Nal^{11}-(*S*)-βMe-NPhe^{6-}	Nasp^{6}	Ndab^{6}	Nlys^{6}
Xaa^{11}	4.7	4.6	4.1	4.5	4.4	3.6	2.9	4.7	4.7	4.4	1.9	3.3	2.5
Phe^{7}	3.0	4.2	2.3	3.6	0.8	2.4	0.8	2.7	−0.3	1.6	0.4	1.3	2.5
D-Trp	4.8	6.8	4.8	4.3	4.9	4.7	4.7	5.0	4.7	4.7	5.1	4.8	4.2
Lys	4.7	4.3	4.9	4.8	5.3	4.9	4.3	4.9	5.1	4.4	4.8	5.5	5.1
Thr	0.6	−0.7	0.5	0.9	0.3	0.4	1.2	−0.4	−0.3	0.1	0.7	0.1	1.3
cis/*trans* Ratio	1.7	1.6	1.4	3.5	0.6	1.4	0.4	2.5	0.5	2.3	2.5	1	1.3

within this turn structure seems to be considerably more stable in compounds containing the (*R*)βMeNphe residues in the bridging region. For the **Nphe^6-Nal^7** compound there are some additional NOE's observable, a medium NOE between TrpNH and Nal^{7}NH and a weak NOE between Phe^{11}NH and ThrNH. These NOEs can be useful to distinguish between the 'folded' and 'flat' conformations since the distances between these protons are different in the folded and flat conformation. The **Nasp^6** compound has a third NH proton with a low temperature dependence, the Phe^{11}NH. This supports a conformation which is 'folded' about Thr. These 'folded' conformations involve a γ-turn about Thr, formed by a hydrogen bond between Phe^{11}HN and LysO.

The side chain orientations are relatively flexible except for the Lys side chain which generally adopts g- and the D-Trp side chain which prefers a *trans* orientation. In the **Nphe^6-Nal^7**-compound and in the compound containing (*R*) or (*S*)β-MeNphe residues in position 6 as well as Nal in either 7 or 11, the Lys and the D-Trp side chains are forced in close spatial proximity as evidenced by several NOEs between these two side chains. For these compounds there are NOEs observable between the Trp aromatic proton H2 and the Lys γ protons, between the Trp aromatic NH and Lys ϵ protons and between the Trp aromatic NH and Lys δ.

Computer simulations of our analogs resulted in general in two conformational families which were both consistent with the NMR data, a 'folded' structure with a C^7 conformation around Phe^7 and Thr^{10} and a 'flat' conformation. Both conformations contain a type II′ β-turn with D-Trp in the i+1 position and a type VI β-turn spanning the residues Xaa^{11} and the peptoid residue. For the Nphe^6 analog, another 'folded' structure was found, in which the bridging region around residues 11 and 6 can be described as 'puckered-up' compared to the other 'folded' conformation (Fig. 3). This conformation also contained a type II′ β-turn with D-Trp in the i+1 position and a type VI β-turn spanning residues Xaa^{11} and the Nphe residue. No such conformation was observed for the Nnal^6 analog.

The 'folded' structures are generally lower in energy than the 'flat' conformations because of the energy contribution of two additional hydrogen bonds under the conditions of the modeling (no solvent molecules). The main differences in the torsional angles between these two families are the ϕ and ψ angles of residues Xcc^7 and Thr. The 'folded' conformations are characterized by a C^7 conformation about these two residues which leads to torsional angles of aproximately $-85°$ (ϕ) and 80° (ψ). These values correspond to a γ-turn about residues 7 and 10. In the flat conformations these values are considerably different and the residues 7 and 10 have ϕ angles of approximately $-155°$ and ψ-angles around $-125°$. While most compounds had similar population of the 'folded' and 'flat' conformation there were two exceptions: the **Nnal^6** analog showed a clear preference for the 'flat' conformation whereas the **Nal^{11}-Nphe** analog did not adopt a 'flat' conformation. For this compound, two 'folded' structures were observed, one highly populated conformation with a C^7 conformation about Thr^{10} and Phe^7 and a less populated conformation which was only 'folded' about Thr^{10}, but not about Phe^7. For the **(*R*)βNMePhe^6-Nal^7** and the **Nal^{11}-(*R*)βNMePhe^6** compound, the concentration of the *cis* conformation was too low to obtain a well defined set of NOE constraints usable for the conformational analysis. As a result, many different poorly defined conformations were observable. The side chain orientation of the peptoid side chain can be described by the torsion angle χ^1 (C^{11}-N6-C^{6}β-C^{6}γ) which adopts values around $-70°$ for the **(*R*)βNMePhe^6** compounds and around $-150°$ for the **(*S*)βNMePhe^6** analogs. The spatial arrangement of the side chain of the peptoid residue results in a considerably closer proximity of the side chains of Xaa^{11} and the aromatic ring of the peptoid residue in the **(*R*)βNMePhe^6** analogs compared to those analogs containing (*S*)βNMePhe^6 residues. The resulting steric effects provide a possible explanation for the different populations of *cis* and *trans* isomers in compounds containing

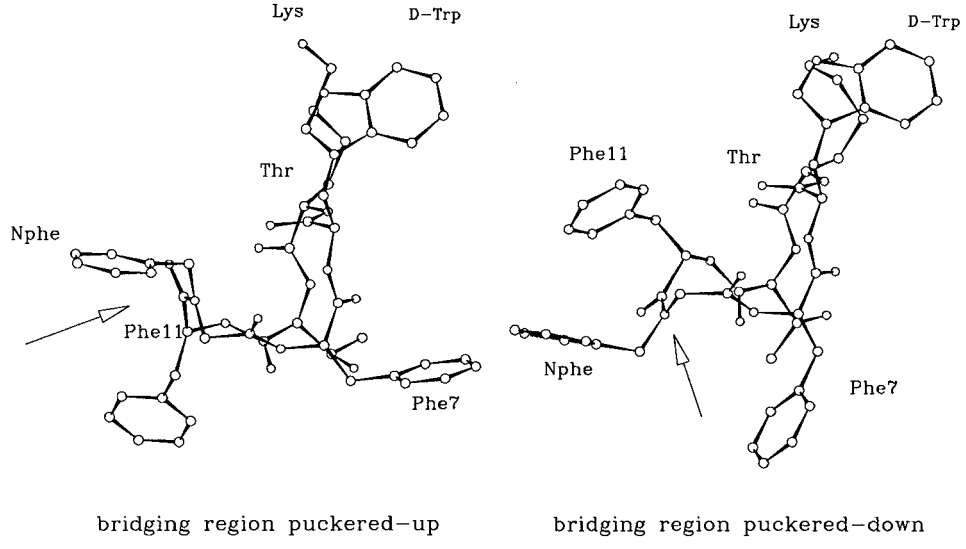

Figure 3. The two 'folded' structures found for the Nphe^6 analog. In the structure on the left the bridging region around residues 11 and 6 can be described as 'puckered-up' compared to the other 'folded' conformation. Both conformations contained a type II′ β-turn with D-Trp in the i+1 position and a type VI β-turn spanning residues Xaa^{11} and the Nphe residue.

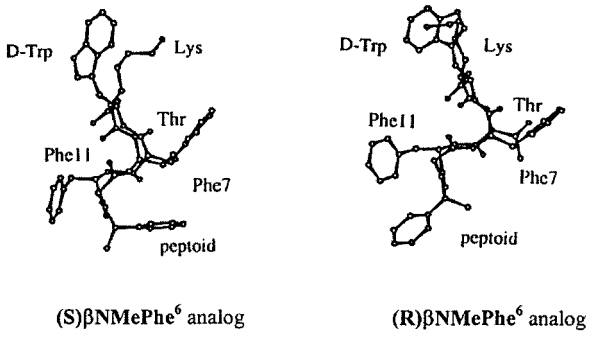

Figure 4. The different orientations of the aromatic ring of the peptoid side chain relative to Phe[11] in the **(*S*)βNMePhe[6]** analog (left) and the **(*R*)βNMePhe[6]** analog (right).

(*R*)βNMePhe[6] and (*S*)βNMePhe[6] residues. The different orientations of the aromatic ring of the peptoid side chain relative to Phe[11] in the **(*S*)βNMePhe[6]** analog (left) and the **(*R*)βNMePhe[6]** analog (right) is shown in Fig. 4. The α-unsubstituted peptoid side chain of the Nphe compounds has considerably more flexibility because of the lack of the constraining chiral methylation and can adopt several different orientations.

Discussion

The variations in bioactivity and selectivity to the hsst2, hsst3 and hsst5 receptors of our analogs compared to L-363,301 suggest that the presence of an additional hydrophobic, basic or acidic group in position 6 can alter the binding to the receptor subtypes. While most of the differences between our compounds are rather subtle there are some important conclusions from these studies:

(1) The binding affinities of the Nasp compound suggest that the presence of a negatively charged residue in the bridging region greatly reduces the binding to the somatostatin receptors even if the compound contains a well defined type II′ β-turn on the opposite side of the ring with an appropriate array of the D-Trp and Lys side chains.

(2) The binding to the hsst2 is not affected by a positively charged residue in the bridging region. This is clear from the binding affinities of the the Ndab and Nlys analogs. Based on the difference between these two compounds, one could potentially expect an increased affinity to the hsst5 and with increasing chain length of a basic residue beyond the four methylene groups in Nlys.

(3) An arylalkyl peptoid residue in close spatial proximity of the Phe[11] side chain might be responsible for the enhancement of selectivity to the hsst2 receptor. This conclusion could be drawn from comparison of the **Nphe**, **(*S*)βMeNphe** and **(*R*)βMeNphe** analogs. The results of these findings and the differences in the side chain orientations within the peptoid residue lead us to propose a model according to which an aromatic peptoid side chain in a parallel arrangement with the Phe[11] side chain such as seen in the **Nphe** and the **(*R*)βMeNphe** compound can be tolerated by the hsst2 receptor but leads to reduced binding activities to the hsst3 and hsst5 receptors. The orientation of the peptoid side chain in **(*S*)βMeNphe** analogs towards the Phe[7] side chain, on the other hand, leads to an overall topology which seems to be less favorable for binding to both, the hsst2 and the hsst5 receptors and results in a lower binding potency to the hsst2 receptor for this compound compared to the other two compounds.

(4) The **(*R*)βMeNphe[6]** analog showed increased in vitro selectivity towards the hsst2 receptor. Based upon these results we envisioned that additional restrictions beyond the methylation in α-position of the accessible side chain orientations in and around the bridging region could further enhance the selectivity of these compounds. The incorporation of Nal into position 7 or 11 of our peptoid analogs was carried out to enhance potency and/or selectivity of these analogs. However, these modifications have reduced the selectivity observed in the first generation of peptoid analogs of L-363,301. The type II′ β-turn region in these molecules is well defined and the parallel orientation and close spatial proximity of the D-Trp and Lys side chains in these compounds can be experimentally observed by the presence of several NOEs between these side chains. Our results suggest that the incorporation of several constrained residues into the bridging region of L-363,301 can overcome the improvements in selectivity achieved by the incorporation of a single side chain constrained residue. Nevertheless, our analogs bind effectively to the hsst2 and hsst5 receptors and the presence of unusual peptoid residues and the Nal residue might improve the bioavailability of our analogs compared to L-363,301.

(5) The incorporation of the Nnal residue in position 6 resulted in an analog which exhibits reduced binding affinity to all hsst receptors but has the best selectivity to the hsst2 receptor in this series of compounds. The observation that this analog preferably adopts the 'flat' conformation while the active but non-selective **Nal[11]-Nphe** analog cannot access the 'flat' conformation could suggest that the 'flat' conformation reduces binding affinity to the hsst receptors but can be tolerated by the hsst2 receptor more than by the others.

Analogs of Sandostatin

The sandostatin analogs D-Phe[5]-c[Cys[6]-Phe[7]-D-Trp[8]-Lys[9]-Xaa[10]-Cys[11]]-Xbb[12]-NH_2 (Xaa=allo-Thr, D-allo-Thr, D-βHyv, βHyv, D-Thr and Xbb=Thr or Xaa=Thr and Xbb=allo-Thr, D-allo-Thr, βHyv, D-Thr) contain subtle variations in the Thr residues in positions 10 and 12. The goal of this study was to examine the effect of these stereochemical changes and methylation on conformation and binding affinity. The sandostatin analogs are listed in Table 5.

The peptide sequences were built up on solid support, using either methyl-benzhydrylamine (MBHA) or Rink amide resin using Fmoc chemistry. After the synthesis of the linear peptide was completed, the N-terminal Fmoc group was removed, and the peptide was cyclized by treatment with excess I_2 in DMF. The cyclized peptide was cleaved from the resin using standard anhydrous HF protocols for the MBHA resin or TFA in case of Rink amide resin. Purification via RP-HPLC, followed by lyophilization yielded the

Table 5. Sandostatin analogs

Compound	Abbreviation
D-Phe^5-c[Cys^6-Phe^7-D-Trp^8-Lys^9-Thr^{10}-Cys^{11}]-L- Thr^{12}-NH_2	**Sandostatin® amide analog**
D-Phe^5-c[Cys^6-Phe^7-D-Trp^8-Lys^9-Thr^{10}-Cys^{11}]-L-allo-Thr^{12}-NH_2	**allo-Thr^{12} analog**
D-Phe^5-c[Cys^6-Phe^7-D-Trp^8-Lys^9-Thr^{10}-Cys^{11}]-D-Thr^{12}-NH_2	**D-Thr^{12} analog**
D-Phe^5-c[Cys^6-Phe^7-D-Trp^8-Lys^9-Thr^{10}-Cys^{11}]-βOH-Val^{12}-NH_2	**β-Hyv^{12} analog**
D-Phe^5-c[Cys^6-Phe^7-D-Trp^8-Lys^9-Thr^{10}-Cys^{11}]-D-allo-Thr^{12}-NH_2	**D-allo-Thr^{12} analog**
D-Phe^5-c[Cys^6-Phe^7-D-Trp^8-Lys^9-L-alloThr^{10}-Cys^{11}]-Thr^{12}-NH_2	**allo-Thr^{10} analog**
D-Phe^5-c[Cys^6-Phe^7-D-Trp^8-Lys^9-D-alloThr^{10}-Cys^{11}]-Thr^{12}-NH_2	**D-allo-Thr^{10} analog**
D-Phe^5-c[Cys^6-Phe^7-D-Trp^8-Lys^9-D-Thr^{10}-Cys^{11}]-Thr^{12}-NH_2	**D-Thr^{10} analog**
D-Phe^5-c[Cys^6-Phe^7-D-Trp^8-Lys^9-βOH-Val^{10}-Cys^{11}]-Thr^{12}-NH_2	**β-Hyv^{10} analog**
D-Phe^5-c[Cys^6-Phe^7-D-Trp^8-Lys^9-βOH-D-Val^{10}-Cys^{11}]-Thr^{12}-NH_2	**D-βHyv^{10} analog**

pure peptides. As an example, the synthesis of [alloThr^{12}] analog is presented in Fig. 5.

The binding affinities of these compounds as presented in Table 6 have been obtained under the same conditions as those for the analogs of L-363,301 containing a peptoid residue. Not unexpectedly, the cyclic octapeptide analogs, exhibit binding to the hsst2, hsst3, and hsst5 receptors, with little or no affinity for the hsst1 or hsst4 receptors. The Thr-amide analog **sandostatin® amide** retains activity at hsst2 and hsst5 relative to octreotide, with a loss of binding to the hsst3. The analogs that contain D-amino acids in position 10 such as **D-Thr^{10}**, **D-βHyv^{10}** and **D-alloThr^{10}** had drastically reduced activity. The **alloThr^{10}** analog maintained activity at all receptors while significantly increasing the activity at hsst1. Both the **βHyv^{12}** and **alloThr^{12}** compounds showed reduced binding affinity at hsst3 compared to octreotide, and increased affinity relative to **sandostatin® amide**, without dramatic changes in the activity at the other receptors.

All analogs with (*S*) configuration at position 10 exhibit high affinity for hsst2 and hsst5 receptor subtypes, whereas the affinity for hsst3 receptors was usually about 5–10 fold lower (except for **sandostatin® amide** which shows about 50 fold less affinity at hsst3). The compounds can generally be described as selective receptor ligands with the selectivity profile hsst2>hsst5>hsst3.

The sandostatin analogs with (*S*) configuration at the C^α in position 6 show great similarity amongst each other and compared to sandostatin®. This is illustrated in Table 7 which gives the chemical shifts of these analogs. Other NMR data such as medium NOEs between the NH protons of Xaa^{10} and Lys and the absence of NOEs between the NH protons of Lys and D-Trp suggest a type II′ β-turn with D-Trp in the i+1 position for all compounds with (*S*) configuration. This is consistent with the low temperature coefficients of the Xaa^{10}NH protons and with strong sequential NOEs between LysNH and TrpH^α medium NOEs between Xaa^{10}NH and LysH^α and medium NOEs between LysNH and LysH^α. The ^{1}H NMR data observed for the analogs with (*R*) configuration at the C^α in position 10 are very different from those observed for those compounds with (*S*) configuration at the C^α in position 10 suggesting that the backbone conformation is considerably changed after incorporation of a D-residue into this position. In particular, these molecules cannot adopt a type II′ β-turn around residues D-Trp and Lys. The NH^9–NH^{10} NOE is absent, the Xaa^{10}NH temperature coefficients are high and the temperature coefficients of the NH protons of Cys^{11} and Thr^{12} are low. The $H^{\alpha 6}$–$H^{\alpha 11}$ (NOEs between the α-protons of the two Cys residues)

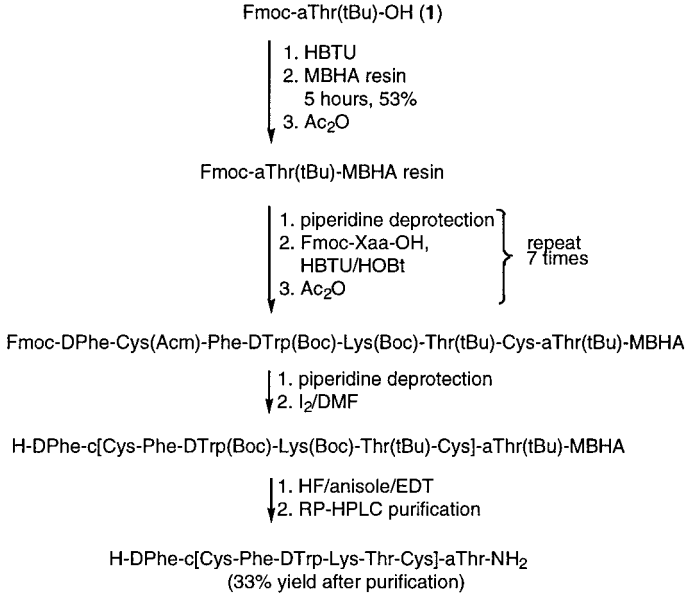

Figure 5. Synthesis of the [alloThr^{12}] analog.

Table 6. In vitro inhibition of radioligand binding to human recombinant receptors: K_i (nM) ±SEM (binding assays were carried out with cell membranes from CHO-K1 cells)

Analogs	hsst1	hsst2	hsst3	hsst4	hsst5
Sandostatin®	875	0.57±0.06	26.8±7.7	>1000	6.78±0.96
1. Sandostatin® amide	761	0.1±0.1	1652±652	>1000	8.4±6
2. [alloThr]^{12}	>1000	1.0±0.2	225±194	>1000	8.8
3. [D-Thr]^{12}	>1000	7.1±0.9	28.9±8.4	>1000	243±160
4. [βHyvVal]^{12}	>1000	0.5±0.1	106±79	>1000	25.7±5
5. [D-alloThr]^{12}	>1000	5.32±0.51	16.5±12.9	>1000	42±24
6. [alloThr]^{10}	693	2.1±1.6	20.1±14.6	>1000	2.3±0.8
7. [D-alloThr]^{10}	>1000	637±254	>1000	>1000	734±267
8. [D-Thr]^{10}	>1000	>1000	>1000	>1000	>1000
9. [βHyvVal]^{10}	>1000	2.8±0.3	85.5±27.2	>1000	139±61

transannular NOEs are weak for analogs containing (*R*) configuration compared with the strong NOEs for those with (*S*) configuration. The chemical shifts also indicate that the backbone conformation has been changed by incorporating a residue with (*R*) configuration at the C^{α} in position 6. This is indicated by the NH chemical shifts of Cys^{6}NH, Cys$^6H^{\alpha}$, Phe^{7}NH, D-Trp^{8}HN, D-Trp$^8H^{\alpha}$, Lys^{9}HN, Lys$^9H^{\gamma}$, Xaa^{10}NH, Xaa$^{10}H^{\alpha}$, Cys$^{11}H^{\alpha}$ and Cys^{11}NH (Table 6). The chemical shifts of the Lys$^9H^{\gamma}$ protons are very instructive since it has been postulated that an upfield shift of these protons in active somatostatin analogs relative to the chemical shifts of these protons in a random coil structure is due to the close spatial proximity of the D-Trp^4 and Lys^5 side chains within the type II′ β-turn. This upfield shift of the Lys$^9H^{\gamma}$ is observable in the analogs with (*S*) configuration at the C^{α} in position 6 (δ=0.8) but not in those compounds with (*R*) configuration at the C^{α} in position 6 (δ=1.13) (Table 6). The chemical shift of these and other protons could possibly be useful in an initial screen for active and inactive compounds.

Other NMR data such as the coupling constants $J_{HN-H\alpha}$ are important indicators of the backbone conformation. For our analogs containing (*S*) configuration in position 10, these coupling constants are large with the exception of $J_{HN-H\alpha}$ (D-Trp) indicating an extended β-sheet conformation. For the **D-Thr^{10}**, **D-allo-Thr^{10}** and the **D-βHyv^{10}** analogs the $J_{HN-H\alpha}$ for most residues are around 7 Hz indicating that

Table 7. Chemical shifts of the sandostatin analogs **4** (β-**Hyv^{12}** analog), **2** (**allo-Thr^{12}** analog), **5** (**D-allo-Thr^{12}** analog), **3** (**D-Thr^{12}** analog), **6** (**allo-Thr^{10}** analog), **9** (β-**Hyv^{10}** analog), **7** (**D-allo-Thr^{10}** analog)), **8** (**D-Thr^{10}** analog) and (β-**D-Hyv^{10}** analog). Values are given in ppm relative to internal DMSO-d_6 (2.49 ppm)

Analog	βHyv^{12}	L-allo-Thr^{12}	D-allo-Thr^{12}	D-Thr^{12}	L-allo-Thr^{10}	βHyv^{10}	D-allo-Thr^{10}	D-Thr^{10}	βD-Hyv^{10}	sandostatin NH$_2$
D-Phe^{5}NH	8.02	8.11	8.08	8.08	8.01	7.96	8.09	8.10	8.08	8.03
Hα	4.18	4.23	4.23	4.24	4.17	4.19	4.17	4.17	4.14	4.21
Hβ	3.25/2.92	3.24/2.90	3.15/2.95	3.19/2.95	3.26/2.95	3.28/2.98	3.06/2.91	3.04/2.91	3.05/2.88	3.25/2.97
	9.28	9.27	9.12	9.14	9.26 Cys^6 NH	9.32	8.68	8.68	8.69	9.23
Hα	5.32	5.26	5.11	5.14	5.40	5.36	4.64	4.64	4.64	5.27
Hβ	2.85/2.81	2.81/2.81	2.79/2.79	2.80/2.78	2.84/2.84	2.83/2.83	2.83/2.71	2.79/2.71	2.89/2.72	2.81/2.81
Phe^7 NH	8.55	8.50	8.45	8.50	8.77	8.65	8.34	8.39	8.35	8.53
Hα	4.64	4.64	4.62	4.66	4.71	4.68	4.64	4.64	4.63	4.67
Hβ	2.84	2.80	2.77	2.85/2.83	2.92/2.80	2.82/2.82	2.69/2.58	2.69/2.56	2.69/2.56	2.83/2.83
D-Trp^8 NH	8.76	8.76	8.68	8.71	8.76	8.76	8.31	8.20	8.20	8.75
Hα	4.16	4.16	4.19	4.22	4.20	4.19	4.56	4.65	4.64	4.19
Hβ	2.94/2.71	2.92/2.71	2.91/2.70	2.96/2.74	2.96/2.77	2.96/2.75	2.98/2.84	2.99/2.84	2.96/2.80	2.95/2.71
Lys^9 NH	8.43	8.43	8.46	8.46	8.40	8.40	8.65	8.65	8.52	8.44
Hα	3.97	3.94	3.98	3.98	4.01	4.02	4.03	4.09	4.13	3.99
Hβ	1.68/1.30	1.69/1.27	1.69/1.30	1.72/1.32	1.74/1.27	1.73/1.28	1.54/1.46	1.55/1.48	1.56/1.46	1.69/1.28
Hγ	0.80	0.77	0.85	0.83	0.79	0.79	1.13	1.22/1.14	1.12	0.80
Hδ	1.32	1.32	1.32	1.28	1.31	1.31	1.47	1.48	1.47	1.32
Hϵ	2.57	2.57	2.57	2.58	2.56	2.56	2.69	2.70	2.67	2.55
NH2	7.59	7.59	7.59	7.64	7.60	7.58	7.67	7.68	7.65	7.63
Xaa^{10} NH	7.61	7.61	7.61	7.66	7.58	7.59	8.03	8.16	8.00	7.62
Hα	4.48	4.45	4.44	4.45	4.42	4.68	4.24	4.08	4.11	4.50
Hβ	3.98	3.99	3.72	4.03	3.99	–	3.93	4.15	–	4.01
Hγ	1.04	1.04	1.06	1.07	1.10	1.19/1.16	1.01	1.05	1.11/1.13	1.07
OH	–	4.87	4.94	–	4.92	4.58	–	4.82	4.82	–
Cys^{11} NH	8.51	8.46	8.36	8.41	8.47	8.48	7.87	7.74	7.81	8.45
Hα	5.13	5.04	5.02	5.13	5.23	5.26	4.50	4.50	4.56	5.15
Hβ	2.88/2.78	2.86/2.79	2.93/2.81	2.99/2.88	2.85/2.85	2.86/2.86	3.03/2.83	3.04/2.92	3.05/2.86	2.87/2.87
Xbb^{12} NH	8.20	8.08	7.91	7.94	8.08	8.20	7.52	7.55	7.60	8.05
Hα	4.27	4.22	4.16	4.21	4.24	4.26	4.09	4.11	4.10	4.24
Hβ	–	3.80	3.72	4.06	4.00	4.02	4.03	4.05	4.01	4.03
Hγ	1.18/1.11	1.08	1.05	1.04	1.04	1.06	0.99	1.01	0.99	1.06
OH	–	4.96	5.01	–	–	5.18	–	4.96	4.91	–
NH2	7.65	7.67	7.56	7.46	7.54	7.62	7.09	7.12	7.10	7.52

the backbone structures are considerably more flexible than in those analogs with (*S*) configuration at the C^{α} in position 10.

Detailed multiconformational analysis of sandostatin® suggested that this molecule adopts multiple conformations[21] and that the β-sheet structure cannot explain all experimental data. Conformations which contain a helical fold in the C-terminal portion were suggested based upon HN^{10}-HN^{11} and HN^{11}-HN^{12} NOEs which are consistently violated in the β-sheet structures. An equilibrium between β-sheet structures and partially helical structures can explain these NOEs. Both NOEs are also observable for the **L-allo-Thr^{12}** analog, but the other analogs show variations in the NOE patterns: in the **β-Hyv^{12}** analog, the HN^{7}-HN^{8} NOE is absent and in the **D-Thr^{12}**, **D-allo-Thr^{12}**, **L-allo-Thr^{10}** and the **β-Hyv^{10}** analogs, the HN^{10}-HN^{11} is not observable. The absence of these NOEs could indicate that the helical structures are less populated in these analogs compared with sandostatin or its **L-allo-Thr^{12}** analog. The **D-Thr^{10}**, **D-allo-Thr^{10}** and the **D-βHyv^{10}** analogs have different backbone structures, therefore, the lack of these NOEs is not surprising. However, it is obvious from other experimental data that the β-sheet conformation is not the only conformation accessible for these analogs: the high Phe^{7}NH temperature coefficient in all analogs clearly indicates that this NH proton is solvent exposed while the β-sheet conformation predicts it to be hydrogen bonded to $Xaa^{10}C{=}O$.

Another interesting experimental detail is the presence of NOEs between the D-Trp and Lys side chains which are observable for the **L-allo-Thr^{10}** analog indicating close spatial proximity of the two side chains within the type II′ β-turn. The same NOEs were observed in some of the peptoid analogs of L-363,301.

The results of the computer simulations showed that all compounds with (*S*) configuration at position 10 adopted a type II′ β-turn with D-Trp in the i+1 position and most structures are folded about Phe^{7} and Thr^{10}. For the **L-allo-Thr^{10}** and the **β-Hyv^{10}** analogs, the type II′ β-turn appears to be slightly less stable and additional conformations were observable that contain a distorted β-turn about residues $D\text{-}Trp^{8}$ and Lys^{9}. The structures obtained for **L-allo-Thr^{10}** and **βHyv^{10}** are also less 'folded' than the structures of the other compounds with (*S*) configuration at position 10. As seen for the cyclic hexapeptide analogs, the ϕ and ψ-torsional angles of the residues at positions 7 and 10 are considerably larger in 'flat' structures observed for **L-allo-Thr^{10}** analog compared to the 'folded' structures of the analogs with (*S*) chirality in the position 10.

The introduction of residues containing (*R*) configuration at the C^{α}-carbon into position 10 disrupts the β II′ turn about Trp^{4} and Lys^{5}, which is crucial for the recognition to the somatostatin receptors and these compounds were essentially inactive. Conformational analysis has shown that these analogs either exhibit a β-turn spanning Lys^{9} and $D\text{-}Thr^{10}$ or a γ-turn about Xaa^{10}. These conformations account for the low temperature coefficient of Cys^{11}NH.

Our studies demonstrate that the sandostatin analogs with (*S*) configuration of the C^{α} of the residue at position 10 adopt conformations very similar to each other. The conformations of these compounds are very similar to those adopted by sandostatin. The backbone conformation can be described as an antiparallel β-sheet formation containing a type II′ β-turn around the $D\text{-}Trp^{4}$ and Lys^{5} residues. With the exception of the **L-allo-Thr^{10}** analog and the **β-Hyv** analog the structures are 'folded' about residues 7 and 10. Also, there appears to be more flexibility in the β-turn region for these two analogs than for the other compounds. These peptides are the only analogs in this series that exhibit some binding to the hsst1 receptor and there could be a correlation between the flexibility in the β-turn and γ-turn regions and binding to the hsst1 receptor. Our modeling results have shown that the **L-allo-Thr^{12}** and the **β-Hyv^{12}** analogs have very similar backbone conformations. The main difference between these two analogs is the orientation of the $D\text{-}Phe^{1}$ aromatic side chain relative to the disulfide bridge. In the **L-allo-Thr^{12}** analog and in the other analogs this side chain adopts a *trans* orientation which results in close spatial proximity of the disulfide bridge and the aromatic ring. This orientation has also been reported for sandostatin. In the **β-Hyv^{12}** analog this side chain prefers a *g*- orientation which leads to a more extended conformation in this region. The aromatic side chain of $D\text{-}Phe^{1}$ and the disulfide bridge are further away from each other in this analog.

Finally, the inactive **D-Thr^{10}**, **D-allo-Thr^{10}** and **β-Hyv^{10}** analogs exhibit completely different backbone conformations from those analogs with (*S*) configuration at the C^{α} in position 10. These compounds cannot adopt the type II′ β-turn. Instead, these molecules seem to prefer a β-turn centered around Lys^{9} and Xaa^{10} or a γ-turn about Xaa^{10}. The fact that these do not bind to the somatostatin receptors proves once again the importance of the type II′ β-turn spanning residues D-Trp and Lys for the binding affinity of somatostatin analogs. Furthermore, our ^{1}H NMR studies have demonstrated that the chemical shift of the protons of the residues 7, 8, 9 and 10 which are part of the type II′ β-turn and especially the Lys γ-protons are considerably different in active vs. inactive compounds. These chemical shifts can be used as important indicators for the presence and absence of the type II′ β-turn and could have potential application in screening of active somatostatin analogs.

Summary

Analogs of the cyclic hexapeptide L-363,301 containing *N*-alkylated residues and the active analogs of our sandostatin compounds share common structural motifs. The presence of a well defined type II′ β-turn with the i+1 and i+2 positions occupied by D-Trp and Lys in our active analogs is not surprising since it is well established that the side chain arrangement established by such a turn structure is in fact required for activity. We have confirmed earlier observations by us and others that in an appropriate side chain arrangement within the β-turn structure the D-Trp and Lys side chains are in close spatial proximity. In the ROESY spectrum of our highly constrained peptoid analogs containing bulky Nal residues and in the L-allo-Thr^{10}

sandostatin analog we were able to actually observe NOEs between the D-Trp and Lys side chains. As reported earlier by Freidinger et al.[12] the Lys γ-protons are upfield shifted compared to the resonances in a random coil structure. This was explained by a shielding effect by the D-Trp aromatic system. The observation of these NOEs between the side chains supports this theory. Another confirmation of this side chain arrangement is the comparison of our active and inactive sandostatin analogs. While the Lys protons in the active analogs are upfield shifted, the resonances of those protons in the inactive compounds are very close to the values for the random coil structure.

We have demonstrated that the introduction of D-residues in position 10 of sandostatin analogs is detrimental to the binding affinity and that analogs containing D-configurated residues in that position cannot adopt the type II′ β-turn required for binding. It is obvious that the NMR data of active and inactive sandostatin analogs are considerably different, and these NMR signals could potentially be used as a first screening tool to separate active and inactive compounds.

In both families of compounds we introduced different residues into the bridging region. The bridging region in the cyclic hexapeptides consists of the residues Xaa^{6}-Nxbb^{7}. In sandostatin analogs the bridging region can be defined as D-Phe^{5}-Cys^{6}-Cys^{11}-Xaa^{12}. Our changes in the bridging region did not result in dramatic changes in potency except for the Nasp analog which exhibits only very weak binding to the hsst2 and no detectable binding to the other receptors. However, the subtle changes in selectivity and potency which were achieved by our modifications to the bridging region give valuable insight into desirable features for the future design of new and more selective somatostatin analogs.

We have observed that a hydrophobic stacking of aromatic residues in the bridging region of cyclic hexapeptides can in fact change the hsst2 selectivity. Furthermore, we could show that introduction of positively charged residues in the bridging region can be tolerated and may in fact be useful for the design of hsst5 selective compounds.

Our results show that certain effects can be achieved with rather subtle changes in stereochemistry within residues in the bridging region. Comparison of the **(*R*)-βMeNphe^{6}** and **(*S*)-βMeNphe^{6}** analogs is a very good example for two compounds that are identical except for the stereochemistry of one single carbon in a side chain located in an area of the molecule that is seemingly less important for binding than the β-turn region. Nevertheless, the differences in binding are significant at the hsst2 and the **(*R*)-βMeNphe^{6}** compound is considerably more hsst2 selective than its diastereomer. Incorporation of additional bulky aromatic groups in the same area of the molecule weakened that effect and led to molecules which exhibit very similar affinities.

Overall, the relatively subtle changes have led to variations in activity and selectivity of well studied compounds. These results will provide important guidelines for the design of new somatostatin analogs.

Acknowledgements

We wish to thank the National Institutes of Health (DK 15410) for their support of this research. We are grateful to Dr John Taylor and Dr Barry Morgan (Biomeasure) for the biological assays.

References

1. Brazeau, P.; Vale, W.; Burgus, R.; Ling, N.; Bucher, M.; Rivier, J.; Guillemin, R. *Science* **1973**, *179*, 77–79.
2. Koerker, D. J.; Harker, L. A.; Goodner, C. J. *Engl. J. Med.* **1975**, *96*, 749–754.
3. Gerich, J. E.; Lovinger, R.; Grodsky, G. M. *Endocrinology* **1975**, *96*, 749–754.
4. Patel, Y. C. *Endocrinology* **1974**, *135*, 2814–2817.
5. Reubi, J. C.; Waser, B.; Rengod, G. *Cancer Res.* **1994**, 3455–3459.
6. Johansson, C.; Wisen, O.; Efendic, S.; Uvnas-Wallensten, K. *Digestion* **1981**, *22*, 126–137.
7. Delfs, J. R.; Dichter, M. A. *J. Neurosci.* **1983**, *3* (6), 1176–1188.
8. Veber, D. F.; Freidinger, R. M.; Perlow Jr, D. S.; Palaveda, W. J.; Holly, F. W.; Strachan, R. G.; Nutt, R. F.; Arison, B. J.; Homnick, C.; Randall, W. C.; Glitzer, M. S.; Saperstein, R.; Hirschmann, R. *Nature* **1981**, *292*, 55–58.
9. Bauer, W.; Briner, U.; Dopfner, W.; Haller, R.; Huguenin, R.; Marbach, P.; Petcher, T. J.; Pless, J. *Life Sci.* **1982**, *31*, 1133–1140.
10. Veber, D. F. Peptides, Synthesis, Structure and Function. *Proceedings of the Seventh American Peptides Symposium*; Rich, D. H., Gross, V. J., Eds.; Pierce Chemical Co.: Rockford, IL, 1983, p 345.
11. Veber, D. F. Design and discovery in the development of peptide analogs. In: *Peptides: Chemistry and Biology, Proceedings of the Twelfth American Peptides Symposium*; Smith, J. A., Rivier, J. E., Eds.; ESCOM: Leiden, 1992, pp 3–14.
12. Freidinger, R. M.; Perlow, D. S.; Randall, W. C.; Saperstein, R.; Arison, B. H.; Veber, D. F. *Int. J. Pept. Protein Res.* **1984**, *23*, 142–150.
13. Melacini, G.; Zhu, Q.; Osapay, G.; Goodman, M. *J. Med. Chem.* **1997**, *40* (14), 2252–2258.
14. Huang, Z.; He, Y.-B.; Raynor, K.; Tallent, M.; Reisine, T.; Goodman, M. *J. Am. Chem. Soc.* **1992**, *114*, 9390–9401.
15. He, Y.-B.; Huang, Z.; Raynor, K.; Reisine, T.; Goodman, M. *J. Am. Chem. Soc.* **1993**, *115*, 8066–8072.
16. Wynants, C.; Van Binst, G.; Loosli, H. R. *Int. J. Pept. Protein Res.* **1985**, *25*, 608–615.
17. Wynants, C.; Van Binst, G.; Loosli, H. R. *Int. J. Pept. Protein Res.* **1985**, *25*, 615–621.
18. Wynants, C.; Tourwe, D.; Kazmierski, W.; Hruby, V.; Van Binst, G. *Eur. J. Biochem.* **1989**, *185* (2), 371–381.
19. Pohl, E.; Heine, A.; Sheldrick, G. M.; Dauter, Z.; Wilson, K. S.; Kallen, J.; Huber, W.; Pfaffli, P. J. *Acta Crystallogr.* **1995**, *D51*, 48.
20. Melacini, G.; Zhu, Q.; Goodman, M. *Biochemistry* **1997**, *36*, 1233–1241.
21. Mattern, R.-H.; Tran, T.-A.; Goodman, M. *J. Pept. Res.* **1999**, *53*, 146–160.

22. Tran, T.-A.; Mattern, R.-H.; Morgan, B. A.; Taylor, J. E.; Goodman, M. *J. Pept. Res.* **1999**, *53*, 134–145.
23. Mattern, R.-H.; Tran, T.-A.; Goodman, M. *J. Pept. Sci.* **1999**, 161–175.
24. Tran, T.-A.; Mattern, R.-H.; Morgan, B. A.; Taylor, J. E.; Goodman, M. *J. Pept. Sci.* **1999**, 113–130.
25. Mattern, R.-H.; Tran, T.-A.; Goodman, M. *J. Med. Chem.* **1998**, *41*, 2686–2692.
26. Tran, T.-A.; Mattern, R.-H.; Afargan, M.; Amitay, O.; Ziv, O.; Morgan, B. A.; Taylor, J. E.; Goodman, M. *J. Med. Chem.* **1998**, *41*, 2679–2685.
27. Mattern, R. H.; Zhang, L.; Rueter, J. K.; Goodman, M. *Biopolymers* **2000**, *53* (6), 506–522.
28. Rueter, J. K.; Mattern, R. H.; Zhang, L.; Taylor, J.; Morgan, B.; Hoyer, D.; Goodman, M. *Biopolymers* **2000**, *53* (6), 497–505.